POLITECNICO
MILANO 1863

SCUOLA DI INGEGNERIA INDUSTRIALE
E DELL'INFORMAZIONE

Kinematic and Kinetic Outcomes of Different Tibiofemoral Component Size Combinations in Total Knee Arthroplasty: A Musculoskeletal Modelling Study

Tesi di Laurea Magistrale in
Biomedical Engineering - Ingegneria Biomedica

Eva Cuko, Student ID: 252088

Advisor:
Prof. Tomaso Maria Tobia Villa

Co-advisors:
Prof. William R. Taylor
Dr. Seyyed Hamed Hosseini Nasab

Academic year:
2025-2026

Abstract: Total Knee Arthroplasty (TKA) is considered the gold-standard treatment for advanced-stage osteoarthritis, as it effectively reduces pain and restores knee joint function. Despite the high survival rates of implants, a significant proportion of patients remain dissatisfied after surgery, and different combinations of tibiofemoral component sizes have been suggested as potential contributors to revision risk. Surgeons frequently combine various femoral and tibial sizes to optimize anatomical fit; however, the biomechanical consequences of these combinations are still poorly understood. Previous studies have focused primarily on *in vitro* experiments or finite element (FE) analyses, emphasizing implant mechanical response while providing limited insight into joint kinematics during functional activities. The present study employed musculoskeletal modeling to investigate the effects of different tibiofemoral component size combinations of the Columbus DD total knee prosthesis (Aesculap) on knee kinematics and kinetics during walking and squatting. Musculoskeletal models allow dynamic, subject-specific predictions of joint loads and motions, overcoming the typical limitations of *in vivo* and *in vitro* methods. The results showed that variations of one or two component sizes did not substantially affect knee kinematics or contact loads. However, localized differences in contact pressures were observed, suggesting potential implications for the long-term mechanical integrity of the implant. The absence of significant kinematic differences is likely related to the consistent tibiofemoral congruency of the Columbus DD design, which allows safe combinations of different tibiofemoral component sizes without major biomechanical impact. Overall, this feasibility study provides a good starting point for future research on tibiofemoral component size combinations in TKA and may help inform surgical planning, optimize component size selection, and provide useful insights for manufacturers.

Key-words: TKA, Revision risk, Component Size, Size combinations, MSK modelling, Columbus DD, Knee kinematics, Knee kinetics

1. Introduction

Total Knee Arthroplasty (TKA) is the gold standard surgical treatment for patients with end-stage Osteoarthritis (OA), effectively reducing pain and restoring knee joint function. OA is the primary clinical indication for

TKA, accounting for approximately 94–97% of all procedures [1]. As the most common musculoskeletal disorder worldwide, OA affects millions of individuals, with prevalence expected to rise significantly due to factors such as age, female sex, obesity, and joint trauma. In 2024, about 7.6% of the global population was estimated to be affected by OA, with an anticipated increase of 60–100% by 2050 [2]. This projected growth is expected to lead to a substantial increase in TKA procedures worldwide. Despite being considered a successful procedure, with approximately 82% of implants lasting up to 25 years, 10–30% of patients are dissatisfied after TKA, which may lead to complex and costly revision surgeries. Common causes for revision TKA (rTKA) include aseptic loosening, infection, instability, patellofemoral complications, and pain, leading to increased postoperative risks, longer hospital stays, and higher healthcare costs worldwide [3, 4]. Several studies have examined the influence of tibiofemoral component sizing on revision risk after TKA, showing conflicting results. For instance, one study [5] reported no statistically significant effect of femorotibial size mismatch on outcomes following total knee replacement. In contrast, other investigations have identified mismatched femoral and tibial components as a contributing factor to revision rates after primary TKA. Specifically, when the femoral component is larger than the tibial one, altered contact forces may induce edge loading on the polyethylene insert, potentially accelerating wear and ultimately leading to implant loosening and instability [6, 7]. In clinical practice, surgeons often combine different component sizes to better fit patient anatomy, a practice supported within certain limits by implant manufacturers and clinical guidelines [8]. Despite its frequent use, the biomechanical and clinical consequences of deviating from standard size combinations remain poorly understood, leaving surgeons with some uncertainty when selecting components. The limited number of studies addressing this issue has long been recognized as a notable gap in the literature [9]. To date, most studies examining size mismatches rely on *in vitro* experiments or finite element (FE) analyses focused primarily on implant mechanics such as contact stresses and wear [9–11]. Although valuable, these methods provide limited insight into joint-level kinematics and functional biomechanics during dynamic activities. In contrast, musculoskeletal (MSK) modelling has emerged as an efficient and cost-effective computational approach to simulate TKA mechanics under varied implant designs and surgical conditions, overcoming the limitations of *in vivo* and *in vitro* studies. MSK models offer rapid, patient-specific predictions of joint loads and kinematics, which can support surgical planning and intraoperative decisions [12–14]. Recent multiscale approaches that integrate musculoskeletal (MSK) and finite element (FE) models have enhanced understanding of implant stresses, strains, and wear. However, these studies primarily use MSK-predicted kinematics and kinetics as inputs for finite element analyses, focusing mainly on the mechanical performance of the prosthesis, while providing limited insight into joint-level kinematics and overall knee biomechanics during functional activities [15]. Therefore, it remains clear that the biomechanical relationship between tibiofemoral size combinations and knee joint function is still largely unexplored, particularly using MSK modelling. For this reason, the present study aims to investigate the effects of different Columbus DD (Columbus Deep Dish, Aesculap, Tuttlingen, Germany) tibiofemoral component size combinations on kinematics and kinetics through MSK modelling. The findings could provide valuable insights for optimizing implant size selection, improving surgical outcomes, and informing manufacturers.

2. Materials & Methods

2.1. Experimental data & K5R model

A previously validated subject-specific lower limb musculoskeletal model of a total knee arthroplasty (TKA) patient, who had undergone a cruciate-sacrificing right TKA with a highly congruent Innex FIXUC implant (Innex FIXUC, Zimmer Biomet), was used as the starting point [13]. This base model represented subject K5R from the CAMS-Knee dataset (65 years old, 1.74 m, 95.6 kg) [16]. The CAMS-Knee dataset includes six TKA subjects performing multiple activities of daily living, with six degrees-of-freedom (DoFs) tibiofemoral kinematics reconstructed from video-fluoroscopy, standard gait laboratory data (skin marker trajectories, ground reaction forces, and electromyography), and *in vivo* six-component knee contact forces and moments measured using instrumented tibial implants [17]. For the current study, only level walking and squatting data from the CAMS-Knee dataset were analyzed to focus on representative functional activities, with five motion cycles selected for each task. The K5R base musculoskeletal model included subject-specific bone geometries reconstructed from CT images, 44 muscles spanning the right leg, scaled to the subject's anthropometry, and major knee ligaments represented by nonlinear spring elements, with each ligament's slack length optimized to maintain 2% strain at full extension of the knee [13]. In addition, tibiofemoral and patellofemoral joint kinematics were defined through contact interactions using detailed 3D triangular mesh geometries of the subject-specific implant (Innex FIXUC, Zimmer Biomet) [18], with articular contact mechanics modeled through an elastic foundation model (Young's Modulus = 465 MPa for tibiofemoral, and 165 MPa for patellofemoral contact; Poisson's Ratio = 0.45 for all contact elements) [19, 20].

2.2. Columbus DD baseline model: Modeling Pipeline 1

The aim of this study was to analyze different tibiofemoral size combinations of Columbus DD implant (Columbus Deep Dish, Aesculap, Tuttlingen, Germany) using musculoskeletal modelling. This highly congruent design retains the posterior cruciate ligament (PCL) and maintains consistent articular congruency across tibial insert sizes, supporting more physiological knee kinematics [9]. To this end, a new musculoskeletal model incorporating the Columbus DD implant was generated. Implant CAD geometries corresponding to the matched tibiofemoral size combination (F4T4) were preprocessed and converted into triangular meshes and aligned with the reference Innex FIXUC geometry incorporated in the K5R base model using custom MATLAB scripts. Alignment was performed by minimizing the distances between the corresponding femoral and tibial mesh point clouds. Preservation of the joint line along the vertical axis was ensured by matching the lowest contact points of the femoral and tibial meshes. The aligned implant meshes were then integrated into the base musculoskeletal model while maintaining its structural hierarchy and coordinate system, ensuring overall model consistency. This adapted MSK model was designated as the baseline Columbus DD model, which was subsequently used as the reference to generate additional models representing different tibiofemoral size combinations for subsequent simulations and analyses.

2.3. Simulation Workflow

All simulations were carried out using the Concurrent Optimization of Muscle Activations and Kinematics (COMAK) framework, within the OpenSim environment. The workflow included Inverse Kinematics (COMAK IK), COMAK, and Joint Mechanics tools, with all model creation and simulation management performed in MATLAB. Joint coordinates were first computed using the COMAK IK tool [21], which takes experimental skin marker trajectory data as input and solves a weighted least-squares optimization problem to reproduce experimental kinematics by minimizing distances between virtual and experimental markers [15]. As a result, the IK analysis provided joint coordinates, angular velocities, and accelerations of the primary joint rotations (e.g., knee flexion–extension) [13]. IK results, together with experimentally measured ground reaction forces for each trial, were then used as inputs to the COMAK algorithm [22] to predict tibiofemoral and patellofemoral secondary degrees of freedom (DoFs), including joint translations and secondary rotations, as well as muscle activations, ligament, and knee contact forces throughout the motion. These results were obtained through simultaneous optimization of secondary kinematics, muscle forces, ligament, and articular contact forces, constrained to reproduce primary joint accelerations while minimizing a cost function addressing muscle redundancy (Eq. 1) [13, 18, 23]. The Joint Mechanics tool was then used to compute joint contact forces and contact pressures [24].

$$\min \sum_{i=1}^{n_{\text{muscles}}} V_i(a_i)^2 \tag{1}$$

Eq. 2.1: Cost function minimized by COMAK, defined as the sum of squared muscle activations $(a_i)^2$ weighted according to muscle volume V_i.

2.4. Columbus DD baseline model Verification

For the Columbus DD baseline model, five gait cycles and five squat cycles were simulated and qualitatively compared against *in vivo* measurements available in the CAMS-Knee dataset. The comparison encompassed all analyzed tibiofemoral kinematic and kinetic variables. Tibiofemoral kinematics included knee flexion–extension, adduction–abduction, internal–external rotation, as well as lateral, anterior, and superior translations. Tibiofemoral kinetics comprised medial, lateral, and total contact forces, together with contact flexion, adduction, and rotation moments. A quantitative validation using error-based metrics was not pursued, as the *in vivo* measurements were obtained from a different implant design (Innex FIXUC) and therefore did not provide a fully comparable reference for the simulated model. Instead, a qualitative comparison of temporal trends and peak timings was considered sufficient to verify the physiological plausibility of the Columbus DD baseline model. Simulated cycles were compared with the corresponding *in vivo* measurements on a cycle-by-cycle basis (e.g., simulated cycle 1 versus *in vivo* cycle 1), and agreement was assessed through visual inspection of temporal patterns, peak timing, and baseline offsets. To identify a representative baseline cycle for each activity, the qualitative comparison was extended across all analyzed kinematic and kinetic variables. For both walking and squatting, the recurrence of the same simulated cycle showing the closest qualitative agreement with the *in vivo* data across multiple parameters was evaluated. The cycle most consistently recurring among the majority of variables was selected as the representative baseline cycle for subsequent analyses. A schematic overview of the complete modeling, simulation, and verification workflow is provided in the Appendix (Fig. A1).

2.5. Size Combinations Musculoskeletal Models: Modeling Pipeline 2

Alternative tibiofemoral size combinations were defined based on clinically relevant deviations from baseline, limited to a maximum of one or two sizes. Femoral oversizing was investigated by increasing the femoral component by one (F5T4) and two sizes (F6T4), while tibial undersizing was analyzed by decreasing the tibial component by one (F4T3) and two sizes (F4T2) (Fig. 1). For each configuration, implant CAD geometries were preprocessed to match the coordinate system of the baseline model and converted into triangular meshes, which were then integrated into the baseline Columbus DD model using custom MATLAB scripts. Integration involved aligning the centroids and matching the lowest contact points of the contact surface meshes to preserve the joint line, thereby ensuring model consistency across all size combinations. This also applies to the F4T4 configuration, which provided a Columbus DD baseline model coherent with the new modeling pipeline. Once the four alternative musculoskeletal models and the new baseline model were generated, walking cycle 1 and squatting cycle 3 were simulated for each size configuration to obtain kinematic and kinetic outputs.

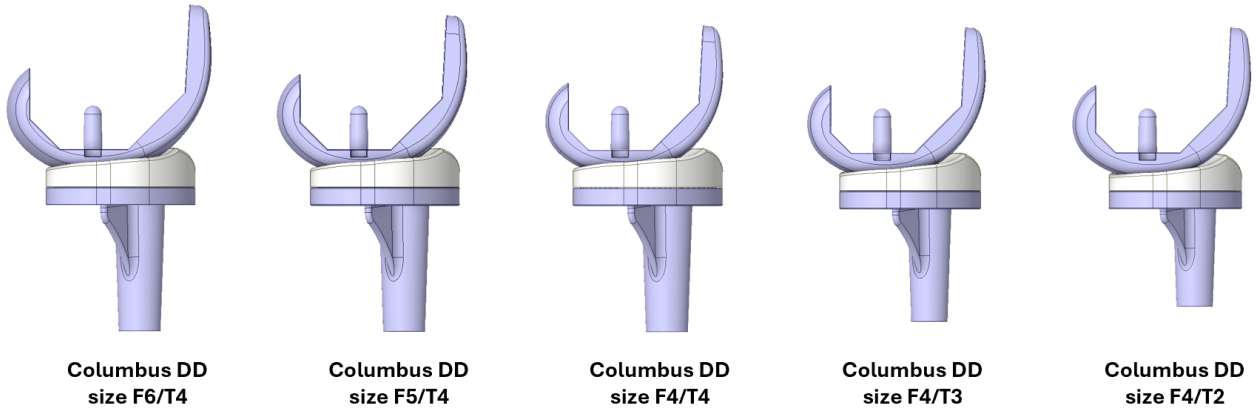

Figure 1: Illustration of the tibiofemoral size combinations investigated.

2.6. Comparison of the results

To evaluate the effects of tibiofemoral size variations, model outputs for each size combination were compared with the Columbus DD baseline (F4T4). A schematic representation of the overall comparison workflow used in this study is provided in the Appendix (Fig. A2). Kinematic and kinetic curves, normalized to 0–100% of the gait cycle for walking and 0–100% of the squat cycle for squatting, were first visually inspected to assess differences relative to baseline. Quantitative deviations were then evaluated using root mean square errors (RMSE). For walking, RMSE was computed over the stance phase (0–60% of the gait cycle), given the higher joint loading occurring during this period, and subphases were examined as needed to capture finer differences. Squatting cycles were instead analyzed over the entire squat cycle. In particular, walking cycles were defined from heel strike to the subsequent heel strike of the instrumented limb, whereas squat cycles spanned from upright standing through deep flexion and back to upright posture. Size combinations showing the largest RMSE values for individual kinematic and kinetic parameters were further analyzed by quantifying peak differences relative to baseline. Peak values were identified as local maxima or minima occurring within the same functional subphase, allowing for small temporal shifts due to changes in motion progression. In addition, configurations presenting notable peak alterations, even in the absence of the highest global RMSE, were considered to support interpretation of the results. For level walking, kinematic analysis focused on adduction–abduction, internal–external rotation, and anterior–posterior translation, as these variables most directly reflect tibiofemoral load distribution and are particularly relevant for evaluating size combination effects. Flexion–extension was largely task-driven and therefore not analyzed, while proximal-distal and medial–lateral translations were excluded due to their minimal functional relevance and susceptibility to model-specific noise. For squatting, the same rationale was adopted, except that proximal–distal translation was included due to its relevance for this activity. Kinetic outcomes comprised medial, lateral, and total contact forces, as well as mean medial and lateral contact pressures. As all simulations were conducted on a single subject and individual motion cycles, the outputs were deterministic, and no statistical analysis could be performed. Therefore, interpretation relied on direct comparison between configurations, emphasizing the observed biomechanical differences.

3. Results

3.1. Baseline Model Verification

For level walking and squatting, cycle 1 and cycle 3, respectively, showed the highest agreement with the *in vivo* measurements and were selected as the representative baseline cycles (Fig. A3, Fig. A4). Peak total contact forces reached approximately 3.0 BW (walking) and 4.0 BW (squatting). Secondary kinematics ranged as follows: adduction-abduction -1° to 2° (walking) and -1° to 1° (squatting); internal-external rotation -10° to 5° (walking) and -10° to -2° (squatting); anterior translation -10 to 5 mm (walking) and -8 to -1 mm (squatting); superior translation 19–22 mm (walking) and 19–24 mm (squatting).

3.2. Size Combinations Results

3.2.1 Walking Kinematics

During level walking, all tibiofemoral size combinations exhibited similar kinematic patterns consistent with the baseline configuration throughout the gait cycle (Fig. 2). Among the six degrees-of-freedom (DoFs) presented in the figure, the following analysis focuses on: adduction–abduction, internal–external rotation, and anterior–posterior translation.

During loading response phase (0–10% of the gait cycle), knee abduction-adduction angles were near 0° at initial contact for all configurations and remained very close to baseline values (Fig. 2, Abduction-Adduction Rotation plot), while external-internal rotation exhibited only minor deviations from baseline with bigger femoral components configurations (F4T5, F4T6) showing slightly lower external rotation, whereas combinations with smaller tibial components (F4T3, F4T2) well tracked baseline curve (Fig. 2, External-Internal Rotation plot). Tibiofemoral anterior–posterior (AP) translation demonstrated a posterior position for all size combinations, consistent with near-full knee extension at heel strike (Fig. 2, Anterior-Posterior Translation plot).

Differences due to size combinations were most pronounced from mid stance to pre-swing (10-60% of the gait cycle). For the abduction–adduction variable, configurations with bigger femoral components (F5T4, F6T4) exhibited greater adduction compared to baseline under load (Fig. 2, Abduction-Adduction Rotation plot). In particular, for F6T4, the average RMSE relative to baseline over the entire stance phase was 0.22°, with a peak difference of -0.35° occurring in pre-swing. In contrast, configurations with smaller tibial components (F4T2, F4T3) showed values closer to baseline, with slightly reduced adduction (Fig. 2, Abduction-Adduction Rotation plot). External-Internal rotation also exhibited size-dependent variations during mid to pre-swing phase. Although the overall rotational trend was preserved across all configurations, F4T2 exhibited increased external rotation (Fig. 2, Internal-External Rotation plot). The average RMSE during the stance phase was 0.59°, with a maximum local RMSE of 1.72° and a peak deviation of -2.01° observed for F4T2 in pre-swing.

For the AP translation variable, combinations with smaller tibial components (F4T2, F4T3) exhibited slightly posterior translation relative to baseline, whereas combinations with larger femoral components remained close (F5T4) to or slightly anterior (F6T4) to baseline values (Fig. 2, Anterior-Posterior Translation plot). During terminal stance, the largest posterior deviation was observed for F4T2, reaching a peak difference of -1.2 mm. In contrast, the F6T4 combination exhibited the highest average RMSE over the stance phase (RMSE = 0.65 mm), with a maximum local RMSE of 1.1 mm observed during pre-swing (Fig. 2, Anterior-Posterior Translation plot). F6T4 also demonstrated the greatest deviation from baseline during the swing phase among all size combinations (Fig. 2, Anterior-Posterior Translation plot). The average RMSE during swing was 1.5 mm, with a maximum local RMSE of 2.1 mm observed in initial swing. Accordingly, the largest peak differences were also recorded for F6T4, respectively of 1.6 mm and 1.2 mm during initial-swing and during mid-swing.

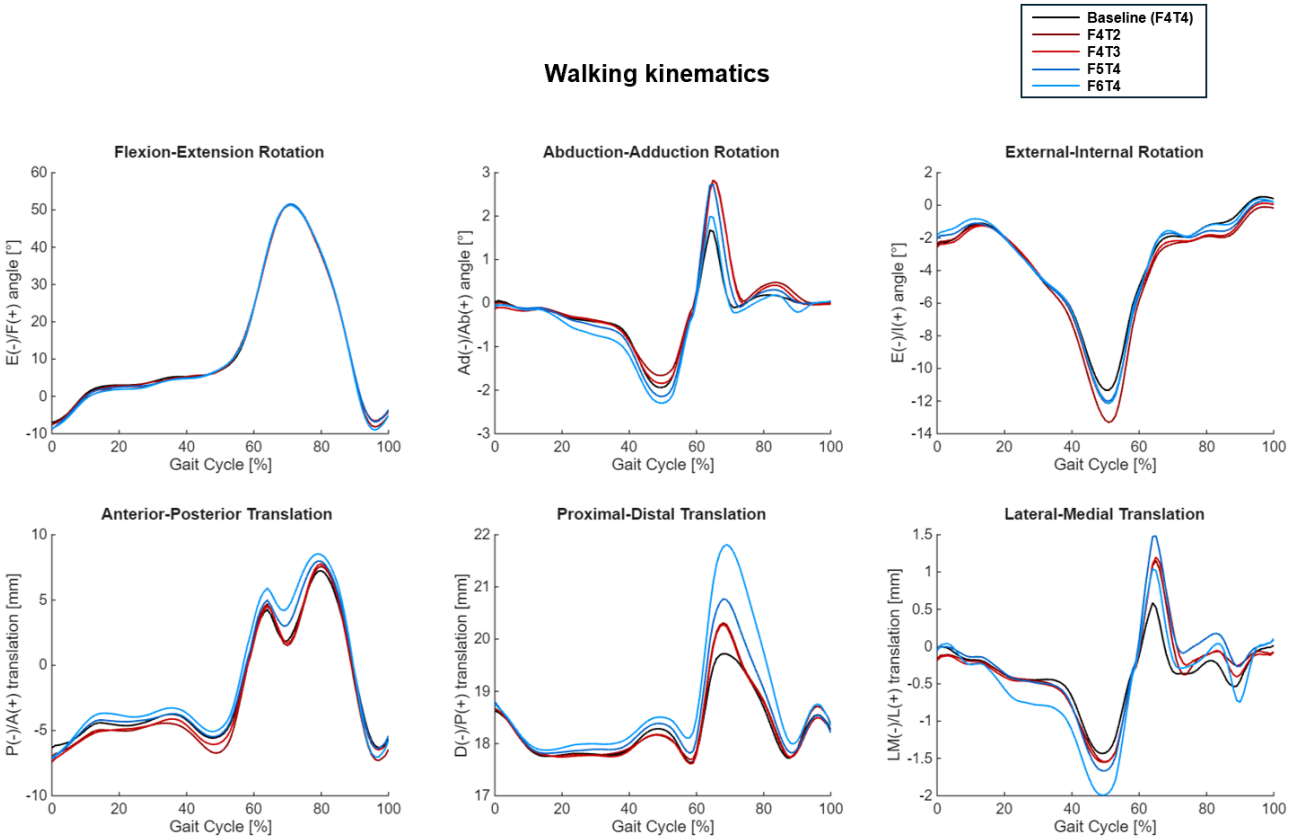

Figure 2: Walking kinematics of all tibiofemoral size combinations showing six degrees-of-freedom (DoFs): flexion–extension, adduction–abduction, internal–external rotation, anterior–posterior translation, proximal-distal translation and medial–lateral translation, plotted over the entire gait cycle (0 to 100%).

3.2.2 Squatting Kinematics

During the squat cycle, all combinations followed the general trends of the baseline knee kinematics, with smaller tibial components showing minimal deviations, while larger femoral components generally exhibited greater deviations (Fig. 3). Among the six kinematic degrees-of-freedom (DoFs) presented in the figure, the following analysis focuses on: adduction–abduction, internal–external rotation, anterior–posterior translation and proximal-distal translation. Regarding abduction–adduction, configurations with smaller tibial components (F4T3, F4T2) closely followed the baseline pattern throughout the squat cycle. In contrast, combinations with larger femoral components (F5T4, F6T4) exhibited increased adduction (Fig. 3, Abduction-Adduction Rotation plot). Notably, F6T4 showed the greatest deviation from baseline, with an overall RMSE of 0.36° and an RMSE of 0.53° during deep knee flexion (45–65% of the squat cycle), where a peak difference of -0.35° was observed. Knee internal–external rotation exhibited reduced external rotation for larger femoral components, with F6T4 showing a RMSE of 0.93° and a maximum peak difference of 1.23° during deep flexion (Fig. 3, External-Internal Rotation plot). For knee anterior-posterior translation, combinations with smaller tibial components (F4T3, F4T2) closely followed baseline, whereas bigger femoral components exhibited greater deviations, showing increased anterior translation (Fig. 3, Anterior-Posterior Translation plot). In particular, F6T4 combination displayed a RMSE over the squat cycle of 2.1 mm, with two peaks differences in descent and ascent phase of 2.7 mm each. For knee proximal-distal translation, smaller tibial component combinations (F4T2, F4T3) showed no difference from the baseline. In contrast, larger femoral component combinations (F4T5, F4T6) exhibited greater deviations, particularly F6T4, which showed a RMSE of 2.68 mm over the entire squat cycle and a peak difference of 4.63 mm during deep flexion, where a maximal proximal translation occurs (Fig. 3, Proximal-Distal Translation plot).

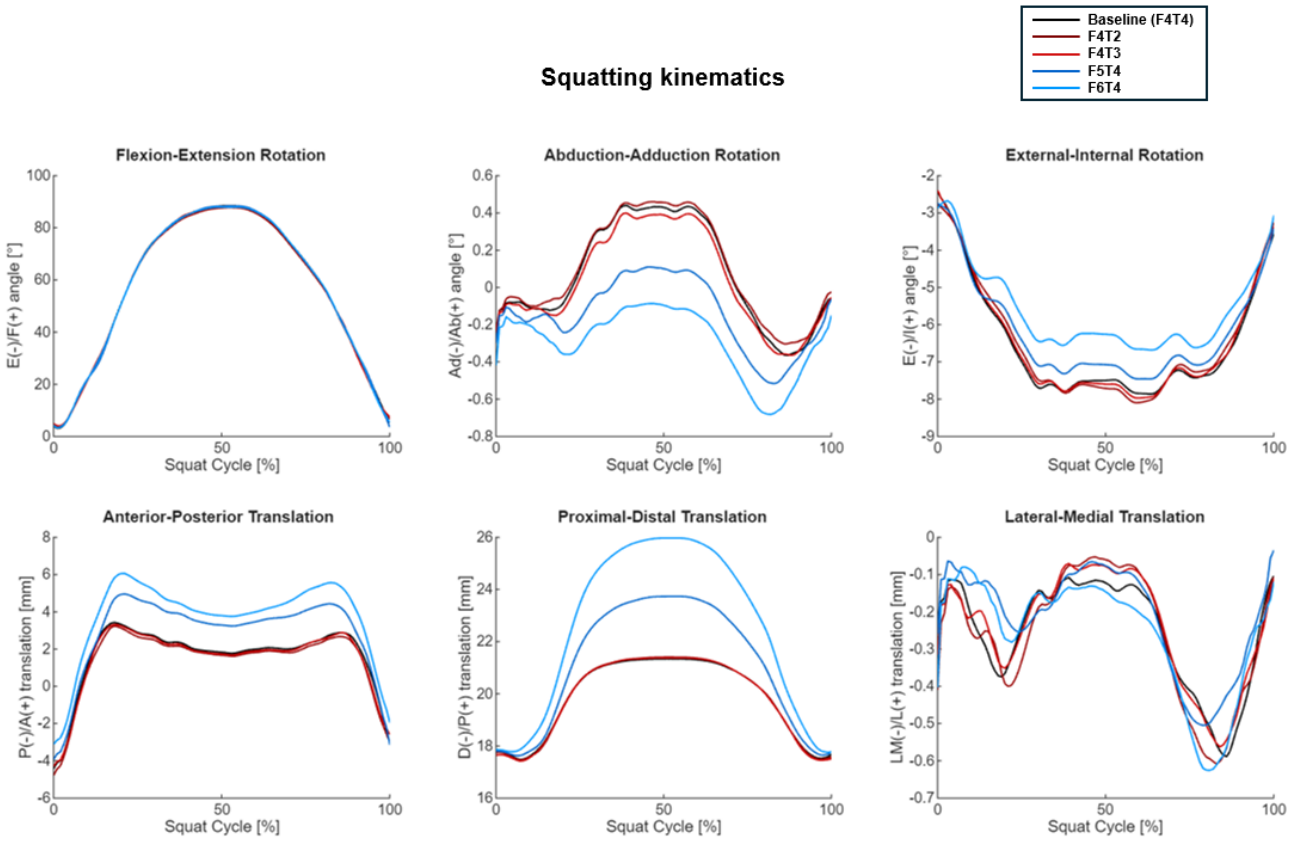

Figure 3: Squatting kinematics of all tibiofemoral size combinations showing six degrees-of-freedom (DoFs): flexion–extension, adduction–abduction, internal–external rotation, anterior–posterior translation, proximal-distal translation and medial–lateral translation, plotted over the entire squat cycle (0 to 100%).

3.2.3 Walking Kinetics

Medial, lateral, and total tibiofemoral contact forces generally followed baseline patterns across all size combinations (Fig. 4). For medial contact force, F6T4 configuration exhibited the largest overall deviation throughout the stance phase (mean RMSE: 0.025 BW), with a maximum local RMSE of 0.064 BW during pre-swing. In the same phase, F6T4 presented the lowest medial peak (peak difference: -0.012 BW), whereas F4T2 configuration showed a slightly higher peak relative to baseline (peak difference: 0.042 BW) (Fig. 4, Medial Contact Force plot). The lateral tibiofemoral contact force was generally comparable to baseline, with small variations in force magnitude across the different prosthetic size combinations during the stance phase. F6T4 configuration exhibited the largest overall deviation across stance, with a mean RMSE of 0.034 BW. Although F4T2 configuration showed the highest local RMSE during the pre-swing phase (0.064 BW), the greatest peak difference in lateral contact force occurred for F6T4 during pre-swing (0.18 BW) (Fig. 4, Lateral Contact Force plot). The total tibiofemoral contact force closely followed baseline values for all prosthetic size combinations, with slightly larger deviations for configurations with increased femoral component sizes. F6T4 configuration exhibited the highest overall deviation, with a mean RMSE of 0.0305 BW across stance phase, a maximum local RMSE of 0.065 BW during pre-swing, and a peak difference of -0.083 BW in the same phase (Fig. 4, Total Contact Force plot).

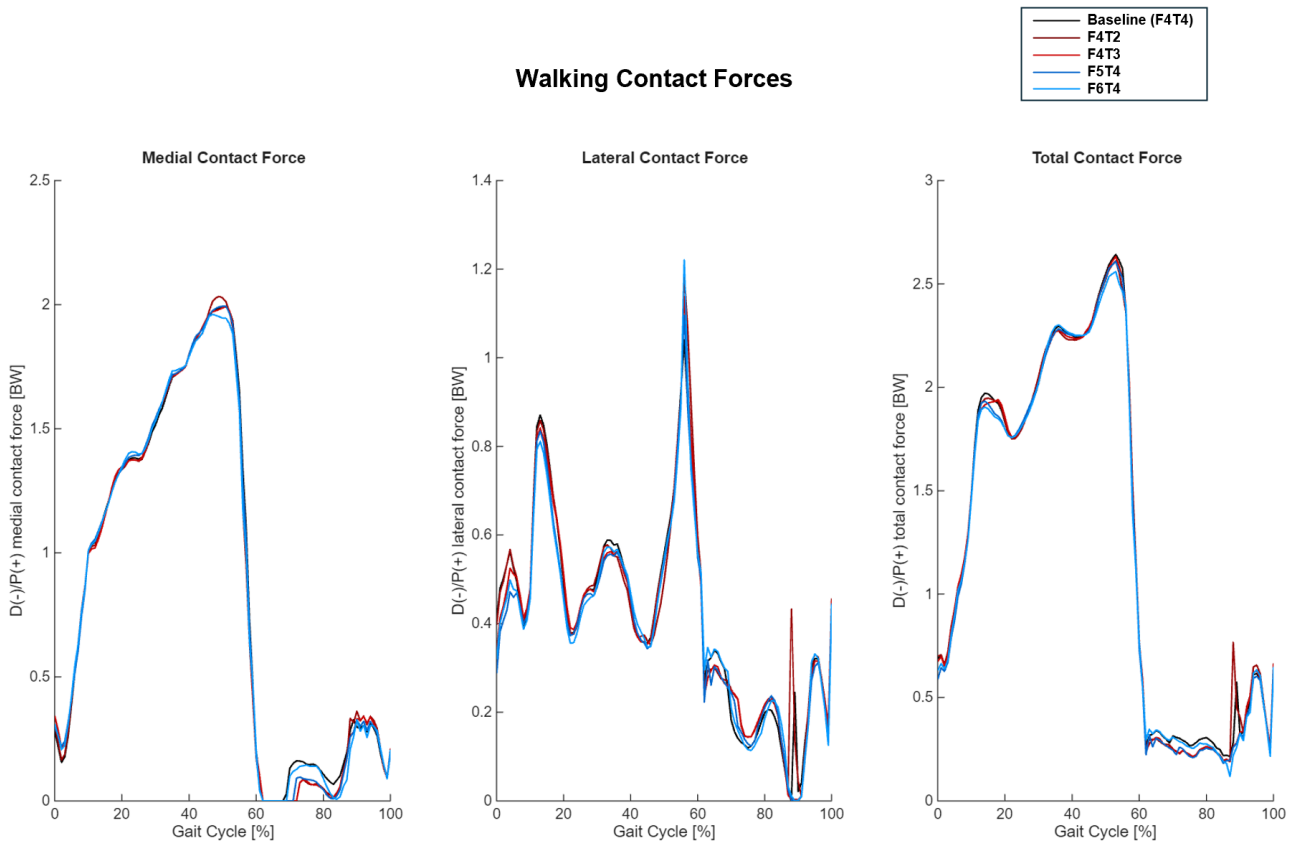

Figure 4: Walking tibiofemoral kinetics of all tibiofemoral size combinations showing medial, lateral and total contact forces plotted over the entire gait cycle (0 to 100%).

Across all prosthetic size combinations, medial and lateral mean contact pressures followed trends similar to those of the baseline, which reached peak values up to 13 MPa on the medial side and 23 MPa on the lateral side (Fig. 5). For medial pressure, configurations with larger femoral components showed a reduction in values throughout stance, whereas combinations with smaller tibial components closely tracked baseline (Fig. 5, Medial Mean Contact Pressure plot). In particular, F6T4 configuration exhibited the largest overall deviation across stance phase (mean RMSE: 2.53 MPa), with a maximum local RMSE of 2.95 MPa and a peak error of 3.0 MPa during terminal stance. For lateral mean contact pressure, larger femoral components combinations showed reduced values during loading response, while smaller tibial components closely followed baseline. Deviations became more pronounced from mid-stance to pre-swing, with F4T2 configuration exhibiting the highest overall deviation (mean RMSE: 2.60 MPa), a maximum local RMSE of 6.72 MPa, and a peak error of 8.15 MPa in pre-swing phase (Fig. 5, Lateral Mean Contact Pressure plot).

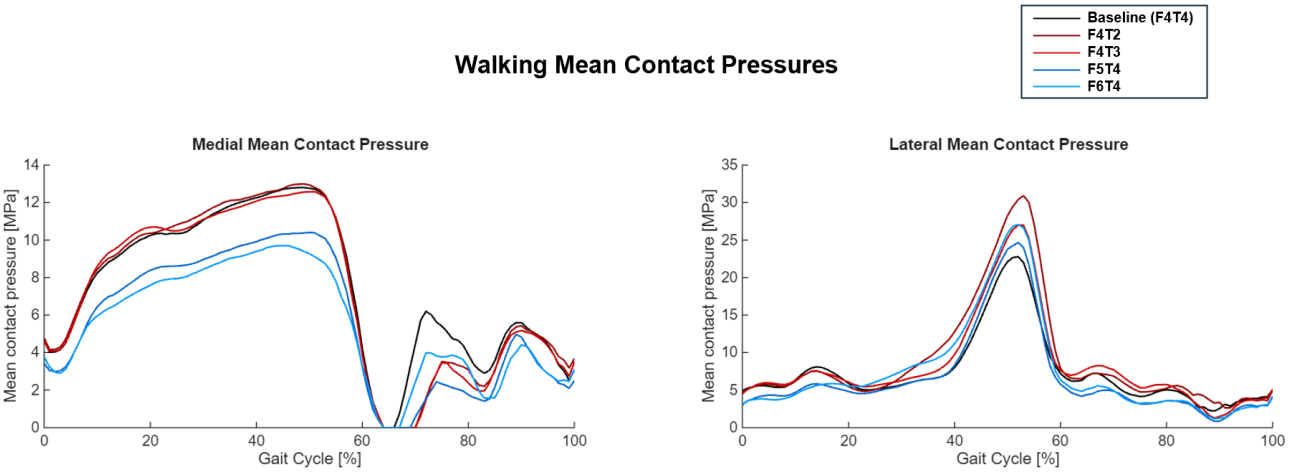

Figure 5: Medial and lateral mean tibiofemoral contact pressures for all size combinations during walking, plotted over the full gait cycle (0–100%)

For the walking activity, tibiofemoral contact pressure distribution was evaluated at the occurrence of the second peak of the total contact force (53% of the gait cycle) (Fig. 6). The pressure distribution in the medial compartment was primarily located in the mid-contact region of the tibial inlay, where the baseline configuration exhibited the highest maximum pressure (27.9 MPa) at this time instant, while F6T4 showed the lowest value among all combinations (21.3 MPa). In the lateral compartment, the maximum contact pressure was observed at the posterior edge of the tibial inlay. In particular, the baseline configuration reached 50.4 MPa, whereas all other size combinations showed increased peak pressures, with F4T2 exhibiting the highest maximum of 69.7 MPa among all tested combinations at the selected time point.

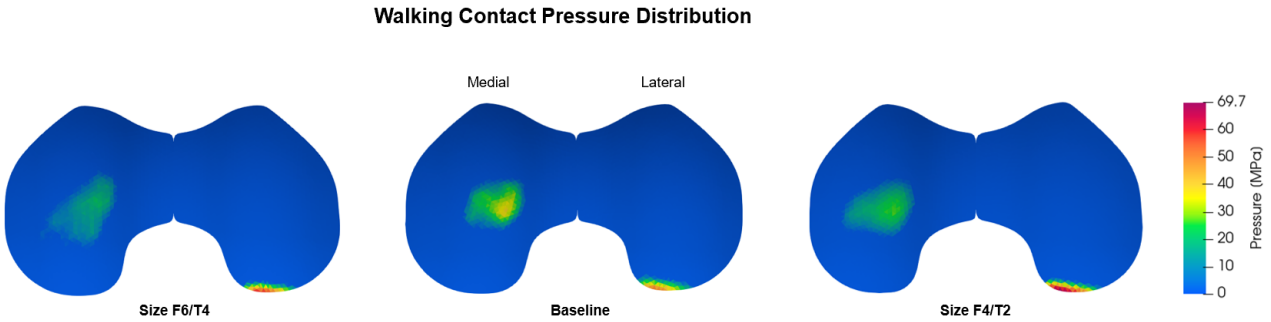

Figure 6: Comparison of tibiofemoral contact pressure maps for the medial and lateral compartments in baseline, F4T2, and F6T4 configurations, shown at the occurrence of the second peak of total contact force during walking (53% of the gait cycle).

3.2.4 Squatting Kinetics

Medial, lateral, and total tibiofemoral contact forces generally followed the baseline patterns across all prosthetic size combinations, with only minor deviations, primarily observed in the central phase of the squat cycle (Fig. 7). The medial contact force showed similar trends across all size combinations, with only minor deviations. In particular, F4T2 exhibited the greatest deviation toward lower values relative to baseline, with a RMSE over the squat cycle of 0.036 BW and a peak difference of -0.07 BW between absolute maxima during the ascent phase Fig. 7, Medial Contact Force plot). A comparable overall behavior was observed for the lateral TF contact force, where all combinations maintained the baseline profile; however, F6T4 exhibited reduced lateral force values and the largest deviation, with an RMSE of 0.15 BW and a peak difference of -0.30 BW between absolute maxima during descent phase Fig. 7, Lateral Contact Force plot). The total TF contact force reflected the same general pattern, with all configurations remaining consistent with baseline but with the two-size mismatch combinations (F4T2 and F6T4) showing greater deviations. In particular, F6T4 demonstrated lower total contact force values, with an RMSE of 0.15 BW and a peak difference of -0.32 BW between absolute maxima during descent phase (Fig. 7, Total Contact Force plot).

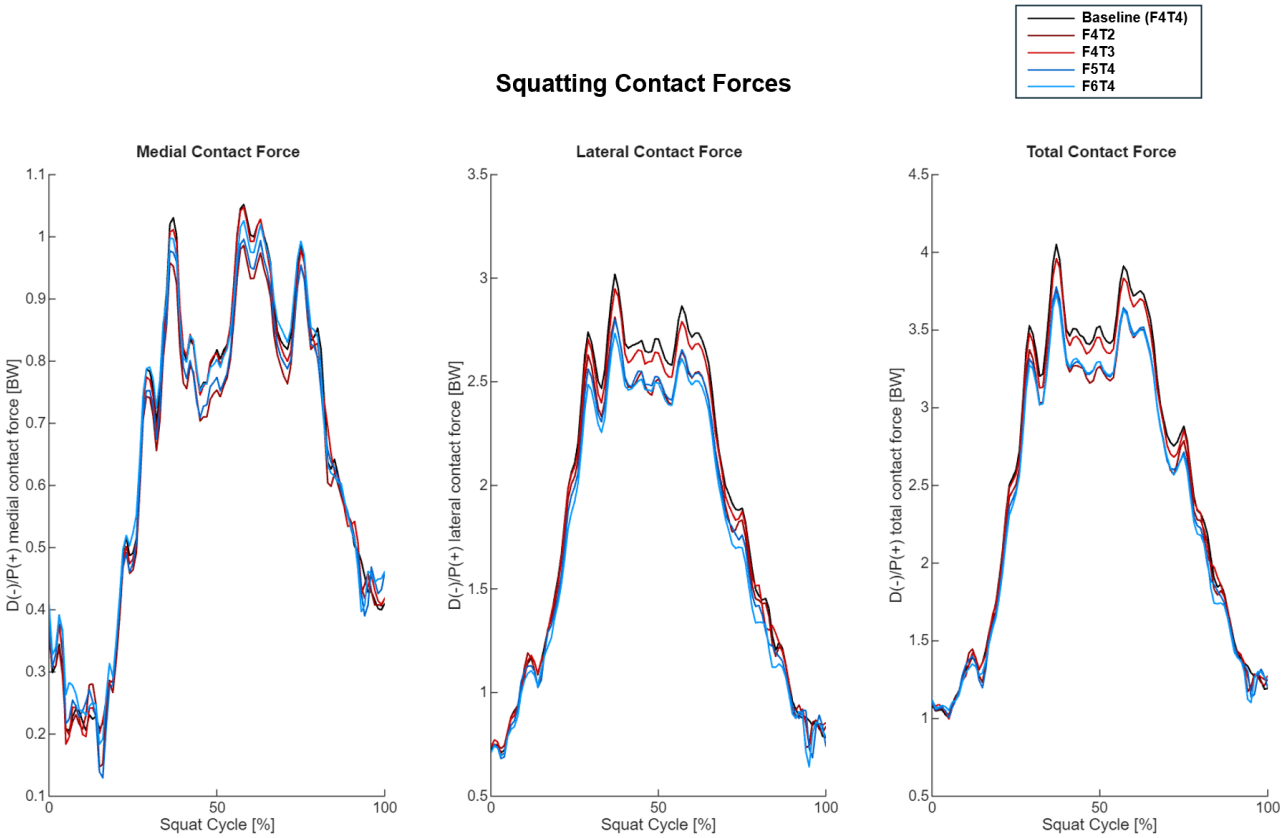

Figure 7: Kinetics of all tibiofemoral size combinations during walking showing medial, lateral and total contact forces plotted over the entire squat cycle (0 to 100%).

Across all prosthetic size combinations, medial and lateral mean contact pressures were generally lower than baseline values, which reached values up to 17 MPa on medial side and 29 MPa on the lateral side (Fig. 8). For the medial contact pressure, the F5T4 configuration showed the largest deviation throughout the squat cycle, with an RMSE of 3 MPa and a peak difference of -4.8 MPa between absolute maxima at the beginning of the ascent phase (Fig. 8, Medial Mean Contact Pressure plot). Regarding the lateral contact pressure, combinations with smaller tibial components (F4T3, F4T2) showed minor deviations from baseline, whereas larger femoral components (F5T4, F6T4) exhibited greater deviations. In particular, F5T4 showed the largest overall deviation, with an RMSE of 4.52 MPa and a peak difference of -6.3 MPa between absolute maxima during the descent phase, whereas F6T4 exhibited the highest local RMSE of 6.6 MPa and a peak difference of -6.3 MPa between absolute minima during the deep knee flexion phase (45–65% of the squat cycle) (Fig. 8, Lateral Mean Contact Pressure plot).

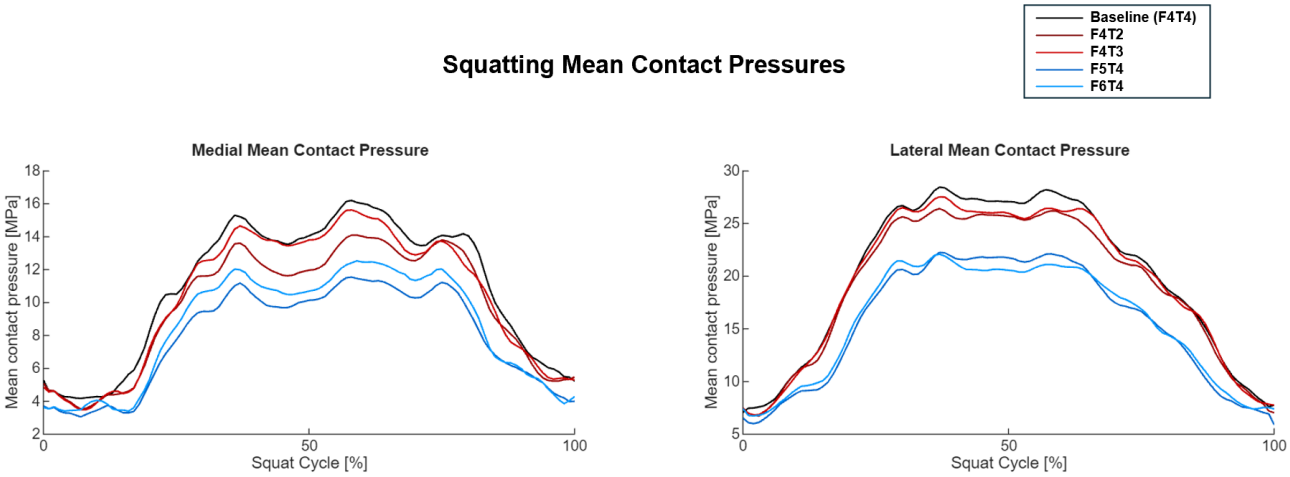

Figure 8: Medial and lateral mean tibiofemoral contact pressures for all size combinations during squatting, plotted over the full squat cycle (0–100%).

For the squatting activity, tibiofemoral contact pressure distribution was evaluated at the largest knee flexion angle (88°). Contact pressures in the medial and lateral compartments were primarily distributed across the

mid-contact region of the tibial inlay, with the lateral compartment slightly shifted posteriorly. The baseline configuration showed the highest maximum pressures in both compartments (Medial = 28.3 MPa, Lateral = 51.8 MPa) (Fig. 9).

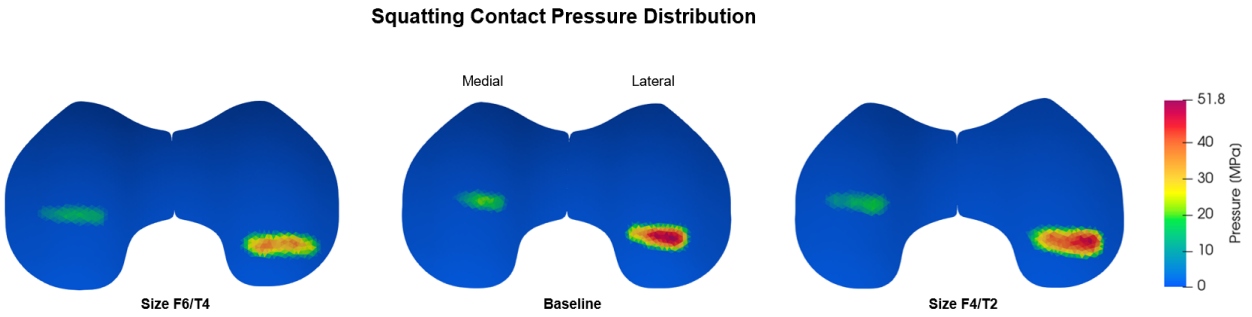

Figure 9: Comparison of squatting tibiofemoral contact pressure maps for the medial and lateral compartments in baseline, F4T2, and F6T4 configurations, shown at the largest knee flexion angle (88°).

4. Discussion

4.1. Baseline model verification

The selected baseline cycles showed comparable overall trends and peak timing relative to the *in vivo* CAMS-Knee measurements for both gait and squat activities, although differences in absolute magnitudes and signal offsets were observed. Such discrepancies are expected given the fundamental geometric differences between the two implant designs (*in silico* Aesculap Columbus DD and *in vivo* Innex FIXUC). Nevertheless, the representative cycles provide a physiologically plausible baseline, as kinematic and kinetic values fall within the ranges reported in the CAMS-Knee dataset [16] and are consistent with findings from other musculoskeletal modeling studies of TKA [15]. Overall, the representative cycles provide a physiologically plausible baseline reference, supporting their use as a standard for evaluating the effects of different size combinations in subsequent analyses.

4.2. Walking Main Findings

The main finding of this study is that variations up to two sizes in tibiofemoral component sizing do not substantially affect knee kinematics in a Columbus DD prosthetized knee joint. During level walking, all tested size combinations closely followed the baseline configuration (Fig. 2), indicating high consistency in joint motion. Deviations in key kinematic variables were minimal, with RMSE values during stance phase generally below 0.6° for abduction-adduction and internal-external rotations, and below 1.5 mm for anterior-posterior translation. Combinations differing by two sizes from the baseline (F6T4 and F4T2) showed slightly more frequent deviations, yet these variations are small relative to physiological ranges and are unlikely to compromise joint stability, functional mobility, or overall gait pattern. Walking kinetics were also largely unaffected by component size variations. Medial, lateral, and total tibiofemoral contact forces closely reproduced baseline patterns across all configurations, with deviations negligible relative to overall joint loading (e.g., total contact force RMSE=0.03 BW). These results suggest that moderate component mismatches of up to two sizes do not significantly affect overall knee kinematics or tibiofemoral joint loading during walking. However, when looking at local contact pressures, they were sensitive to tibiofemoral component size combinations. The smaller tibial configuration (F4T2) exhibited peak lateral mean contact pressures of up to 8.15 MPa during pre-swing, while the larger femoral configuration (F6T4) showed slightly reduced medial mean contact pressures (RMSE = 2.5 MPa) relative to baseline (Fig. 5). Maximum contact pressure in F4T2 was observed on the posterior edge of the lateral compartment (69.7 MPa), whereas F6T4 displayed lower peak maximum contact pressure on medial compartment (Fig. 6). These localized peaks likely result from multiple interacting factors. Cinematically, slight external rotation and posterior translation in smaller tibial components may have shifted the lateral contact posteriorly, while the medial compartment remained centered in the mid-contact region. Additionally, differences in effective contact area, resulting from changed surface conformity across size combinations, could have contributed to the altered local pressure magnitudes. Thus, the observed peak pressures are not solely a geometric effect, but likely reflect the combined influence of altered motion patterns and local contact conditions. As a result, configurations with smaller tibial components promoted higher local peak pressures. The magnitude and location of these peaks may be mechanically relevant: under repetitive loading across many gait cycles,

they could potentially contribute to long-term polyethylene wear, edge delamination, or fatigue-related damage. In contrast, the medial compartment remained more centrally loaded, highlighting that local stress alterations are highly compartment- and configuration-dependent.

4.3. Squatting Main Findings

For squatting, similar considerations to those for walking apply. All size combinations preserved the overall kinematic pattern of the baseline configuration; however, deviations were more pronounced compared to level walking, particularly during deep knee flexion (45–65% of the squat cycle). Larger femoral components consistently showed greater deviations, while smaller tibial components generally remained closer to baseline behavior (Fig. 3). Deviations in key kinematic variables were minimal, with RMSE values generally below 0.93° for abduction-adduction and internal-external rotations, and up to 2.1 mm for anterior-posterior translation and 2.68 mm for proximal-distal translation. These variations are small relative to physiological ranges and are unlikely to compromise overall joint stability or functional mobility during squatting. Squatting kinetics were also largely unaffected by component size variations. Tibiofemoral contact forces largely followed baseline patterns. Even in the two-size mismatch configurations (F4T2 and F6T4), deviations in total contact force were moderate (RMSE up to 0.15 BW; peak difference -0.32 BW). Notably, larger femoral components were associated with slightly reduced lateral and total contact forces (Fig. 7). These results suggest that moderate component mismatches of up to two sizes do not significantly affect overall knee kinematics or tibiofemoral joint loading during squatting. However, when looking at local contact pressures, they were sensitive to tibiofemoral component size combinations: larger femoral components (F5T4, F6T4) tended to reduce both medial and lateral mean contact pressures (medial RMSE up to 3 MPa; lateral RMSE up to 4.52 MPa), whereas smaller tibial components remained close to baseline values (Fig. 8). Notably, the baseline configuration exhibited the highest mean contact pressures among all tested combinations. The reduction in mean pressures for larger femoral components, despite similar total joint contact forces, likely reflects an increase in effective contact area (Fig. 9). Although the baseline configuration may be considered the nominal or standard option, these findings suggest that it does not necessarily represent the most mechanically favorable condition during deep flexion. Indeed, contact pressures may be influenced by differences in articular conformity at specific phases of the activity across the various size combinations. Therefore, the observed reductions in contact pressure are likely attributable to variations in surface conformity introduced by the larger femoral component, which modifies the engagement pattern between the femoral condyles and the tibial inlay, thereby redistributing the load over a broader contact area.

4.4. Comparison with Literature and Clinical Implications

Overall, the results demonstrate that there are no substantial kinematic differences for either walking or squatting, which translates into no significant variations in knee contact loads. This finding is consistent with *in vitro* study on the Columbus DD system [9], which reports that preserved kinematics in squatting is due to the fact that, for this design, congruency remains similar across all size combinations. These results confirm that the common clinical practice of using different femoral and tibial size combinations in the Columbus DD design does not substantially affect knee kinematics, particularly since only clinically relevant size variations (one to two sizes up or down) were analyzed. Consequently, controversial findings regarding the effect of combining different tibial and femoral component sizes on revision rates and clinical outcomes may partly stem from differences in TKA system congruency and the high variability in prosthesis designs. To support this hypothesis, documenting the congruency spectrum and design features of different TKA systems would be valuable when reporting revision rates and clinical outcomes associated with various size combinations [9].

4.5. Limitations and Outlooks

This study has several limitations. First, the observed contact pressures during walking may partly reflect inherent limitations of the elastic foundation model used for articular contact mechanics, which estimates contact pressure based on surface proximity. As a result, peak values at contact boundaries may be overestimated. In light of this limitation, future developments could integrate musculoskeletal (MSK) and finite element (FEA) modeling approaches [15], as the use of subject-specific kinetic outputs from MSK simulations as input to FEA may provide more accurate and physiologically consistent contact pressure predictions. Furthermore, this study is based on a single subject-specific model and includes only one cycle for both walking and squatting, as well as a single prosthesis design. Consequently, inter-subject and intra-subject variability in movement patterns is not captured, which may limit the generalizability of the findings. Regarding the models implementation, although the new prosthesis was aligned with the baseline model and the underlying structure and hierarchy

were preserved among all MSK models created to ensure consistency, further optimization of mesh alignment could be performed. The model is particularly sensitive to mesh definition, especially in regions characterized by complex geometries, which may influence simulation convergence. Additionally, the patellar position within the patellofemoral joint could be further optimized according to the femoral component size considered in the model. Validation of the Columbus DD baseline model was performed against *in vivo* data from Innex FIXUC (CAMS-Knee dataset) using a visual and qualitative approach, which is inherently subjective. Nevertheless, baseline results were consistent with physiological data and thus reliable and since the modelling pipeline was kept consistent among all size combinations, the comparison between the results is reliable. Finally, prosthetic sizing was the only parameter deterministically varied in this study. Given the multifactorial nature of biomechanical interactions affected by component size combinations, including soft tissue behavior, further investigations are warranted to fully capture all biomechanical effects.

5. Conclusions

Using tibiofemoral size combinations differing by up to two sizes did not substantially affect knee kinematics or contact loads during walking and squatting, supporting the safe use of different tibiofemoral size combinations within the Columbus DD system. While contact pressure analysis highlighted localized variations that could potentially influence implant longevity, including long-term wear or edge delamination, further studies are required to better investigate these effects. Overall, this feasibility study provides a good starting point for future research aimed at evaluating the effects of various tibiofemoral size combinations on the kinematics and kinetics of the prosthetized knee joint.

6. Bibliography and citations

References

[1] A. J. Carr et al. Knee replacement. *The Lancet*, 379(9823):1331–1340, April 2012. doi: 10.1016/S0140-6736(11)60752-6.

[2] A. Courties, I. Kouki, N. Soliman, S. Mathieu, and J. Sellam. Osteoarthritis year in review 2024: Epidemiology and therapy. *Osteoarthritis Cartilage*, 32(11):1397–1404, November 2024. doi: 10.1016/j.joca.2024.07.014.

[3] H. Inui, R. Yamagami, K. Kono, and K. Kawaguchi. What are the causes of failure after total knee arthroplasty? *J. Jt. Surg. Res.*, 1(1):32–40, December 2023. doi: 10.1016/j.jjoisr.2022.12.002.

[4] P. Sadoghi, A. Koutp, D. P. Prieto, M. Clauss, M. E. Kayaalp, and M. T. Hirschmann. The projected economic burden and complications of revision hip and knee arthroplasties: Insights from national registry studies. *Knee Surg. Sports Traumatol. Arthrosc.*, 33(9):3211–3217, September 2025. doi: 10.1002/ksa.12678.

[5] S. Heylen, K. Foubert, A. Van Haver, and P. Nicolai. Effect of femoro-tibial component size mismatch on outcome in primary total knee replacement. *The Knee*, 23(3):532–534, June 2016. doi: 10.1016/j.knee.2016.03.003.

[6] Z. G. Brown, A. R. Loch, C. Holder, and C. J. Wall. Does relative femoral and tibial component size influence revision risk following primary total knee arthroplasty? *J. Arthroplasty*, 41(1):125–131, January 2026. doi: 10.1016/j.arth.2025.06.033.

[7] S. W. Young, H. D. Clarke, S. E. Graves, Y.-L. Liu, and R. N. De Steiger. Higher rate of revision in pfc sigma primary total knee arthroplasty with mismatch of femoro-tibial component sizes. *J. Arthroplasty*, 30(5):813–817, May 2015. doi: 10.1016/j.arth.2014.11.035.

[8] K. Tucker et al. Efort recommendations for off-label use, mix & match and mismatch in hip and knee arthroplasty. *EFORT Open Rev.*, 6(11):982–1005, November 2021. doi: 10.1302/2058-5241.6.210080.

[9] I. Dupraz et al. Impact of femoro-tibial size combinations and tka design on kinematics. *Arch. Orthop. Trauma Surg.*, 142(6):1197–1212, June 2022. doi: 10.1007/s00402-021-03923-y.

[10] R. Popescu, E. G. Haritinian, and S. Cristea. Relevance of finite element in total knee arthroplasty - literature review. *Chir. Buchar. Rom. 1990*, 114(4):437–442, 2019. doi: 10.21614/chirurgia.114.4.437.

[11] K.-S. Kang et al. Validation of the finite element model versus biomechanical assessments of dental implants and total knee replacements. *Bioengineering*, 10(12):1365, November 2023. doi: 10.3390/bioengineering10121365.

[12] M. Khasian, B. A. Meccia, M. T. LaCour, and R. D. Komistek. A validated forward solution dynamics mathematical model of the knee joint: Can it be an effective alternative for implant evaluation? *J. Arthroplasty*, 35(11):3289–3299, November 2020. doi: 10.1016/j.arth.2020.06.017.

[13] N. Guo et al. Posterior tibial slope influences joint mechanics and soft tissue loading after total knee arthroplasty. *Front. Bioeng. Biotechnol.*, 12:1352794, April 2024. doi: 10.3389/fbioe.2024.1352794.

[14] P. Tzanetis, M. A. Marra, R. Fluit, B. Koopman, and N. Verdonschot. Biomechanical consequences of tibial insert thickness after total knee arthroplasty: A musculoskeletal simulation study. *Appl. Sci.*, 11(5):2423, January 2021. doi: 10.3390/app11052423.

[15] C. Curreli, F. Di Puccio, G. Davico, L. Modenese, and M. Viceconti. Using musculoskeletal models to estimate in vivo total knee replacement kinematics and loads: Effect of differences between models. *Front. Bioeng. Biotechnol.*, 9:703508, July 2021. doi: 10.3389/fbioe.2021.703508.

[16] W. R. Taylor and et al. A comprehensive assessment of the musculoskeletal system: The cams-knee data set. *J. Biomech.*, 65:32–39, December 2017. doi: 10.1016/j.jbiomech.2017.09.022.

[17] B. Heinlein, F. Graichen, A. Bender, A. Rohlmann, and G. Bergmann. Design, calibration and pre-clinical testing of an instrumented tibial tray. *J. Biomech.*, 40:S4–S10, January 2007. doi: 10.1016/j.jbiomech.2007.02.014.

[18] M. Febrer-Nafría, M. J. Dreyer, A. Maas, W. R. Taylor, C. R. Smith, and S. H. Hosseini Nasab. Knee kinematics are primarily determined by implant alignment but knee kinetics are mainly influenced by muscle coordination strategy. *J. Biomech.*, 161:111851, December 2023. doi: 10.1016/j.jbiomech.2023.111851.

[19] Y. Bei and B. J. Fregly. Multibody dynamic simulation of knee contact mechanics. *Med. Eng. Phys.*, 26(9):777, November 2004. doi: 10.1016/j.medengphy.2004.07.004.

[20] C. R. Smith, K. W. Choi, D. Negrut, and D. G. Thelen. Efficient computation of cartilage contact pressures within dynamic simulations of movement. *Comput. Methods Biomech. Biomed. Eng. Imaging Vis.*, 6(5):491–498, September 2018. doi: 10.1080/21681163.2016.1172346.

[21] T.-W. Lu and J. J. O'Connor. Bone position estimation from skin marker co-ordinates using global optimisation with joint constraints. *Journal of Biomechanics*, 32(2):129–134, February 1999. doi: 10.1016/S0021-9290(98)00158-4.

[22] S. C. E. Brandon, C. R. Smith, and D. G. Thelen. Simulation of soft tissue loading from observed movement dynamics. In *Handbook of Human Motion*, pages 1–34. Springer International Publishing, Cham, 2017. doi: 10.1007/978-3-319-30808-1_172-1.

[23] C. R. Smith, S. C. E. Brandon, and D. G. Thelen. Can altered neuromuscular coordination restore soft tissue loading patterns in anterior cruciate ligament and menisci deficient knees during walking? *Journal of Biomechanics*, 82:124–133, January 2019. doi: 10.1016/j.jbiomech.2018.10.008.

[24] C. Smith. opensim-jam. `https://github.com/clnsmith/opensim-jam`, 2025. C++ source code.

A. Appendix A

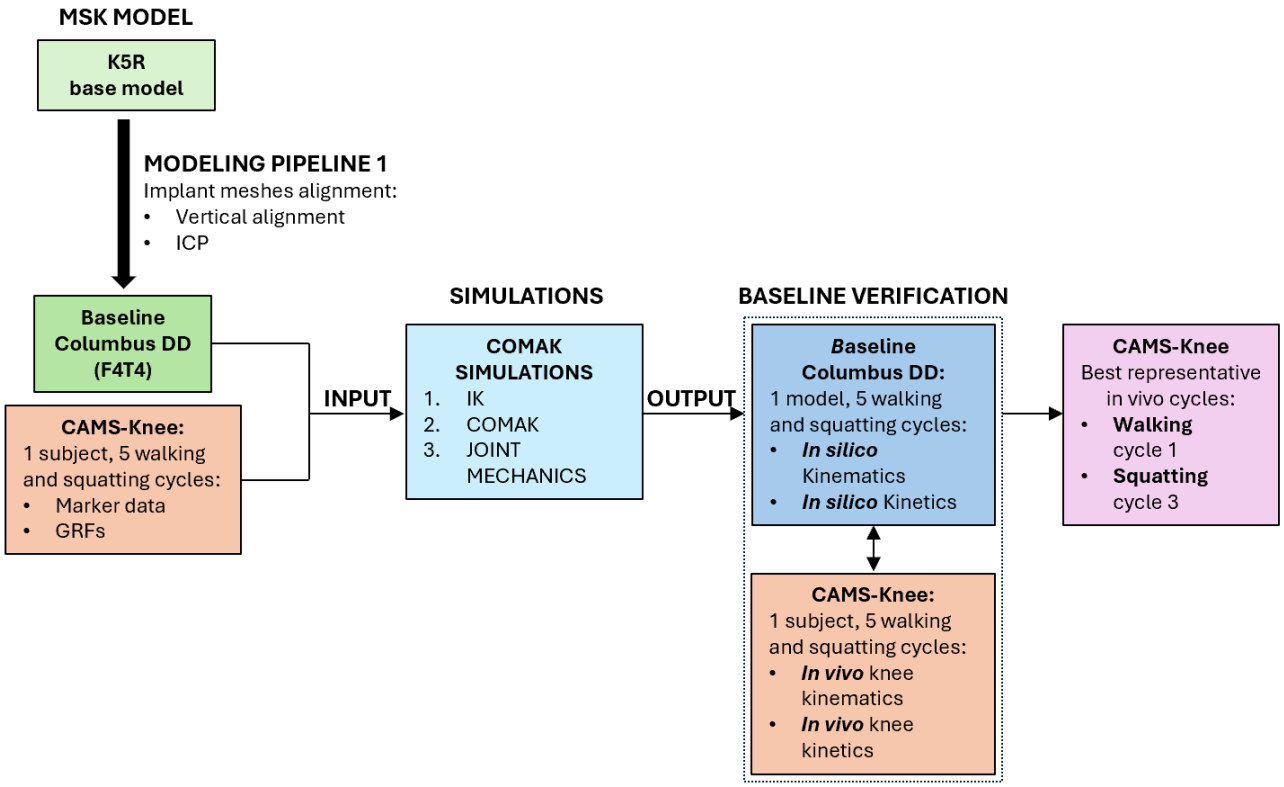

Figure A1: Schematic overview of the complete modeling pipeline, including implant integration, COMAK simulations, and qualitative baseline verification against *in vivo* CAMS-Knee measurements.

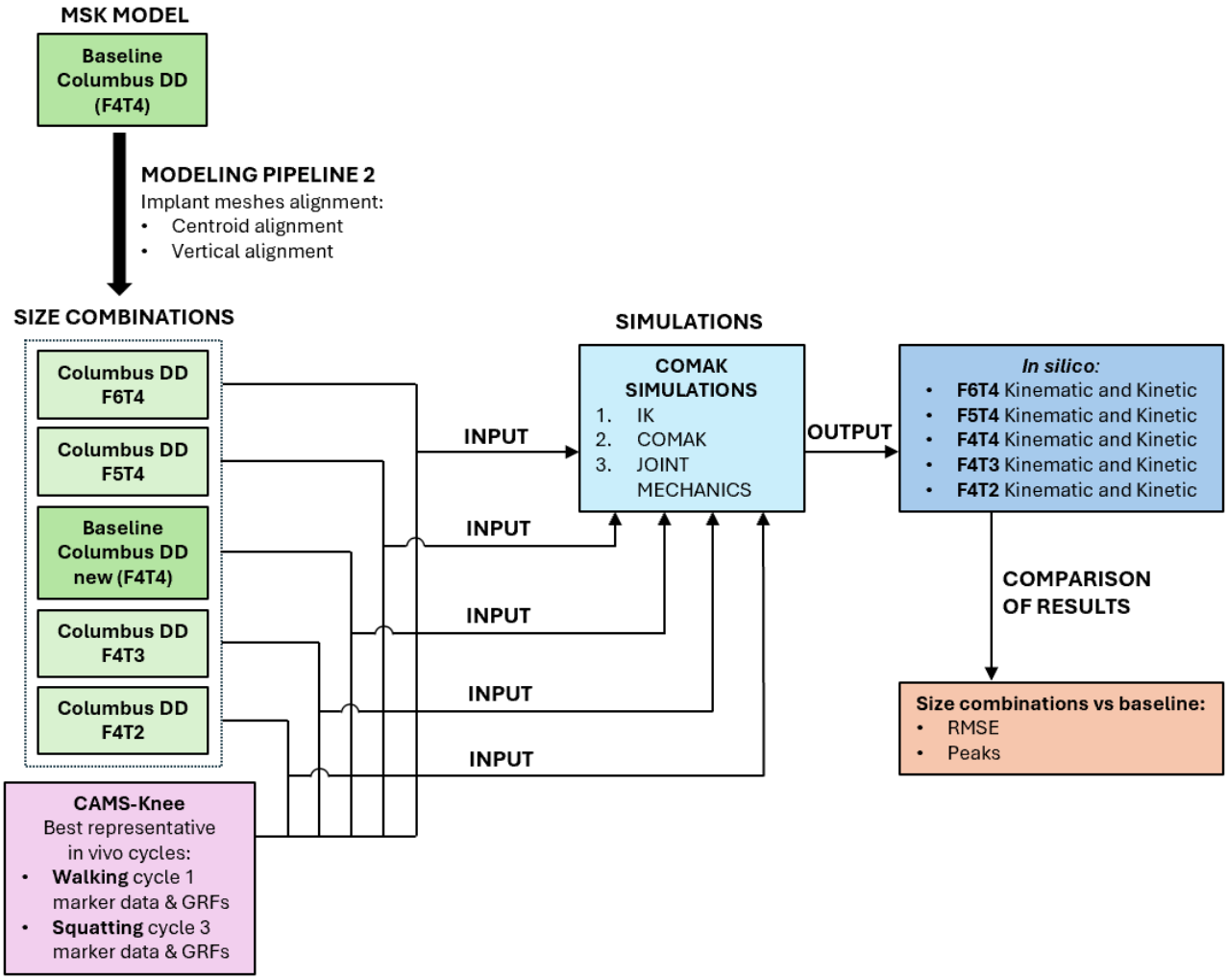

Figure A2: Workflow for the evaluation of different tibiofemoral size combinations. Musculoskeletal simulations were performed using COMAK to obtain kinematic and kinetic outputs, which were subsequently compared with the baseline configuration (F4T4) through inspection of time-normalized curves, RMSE calculation, and peak difference analysis.

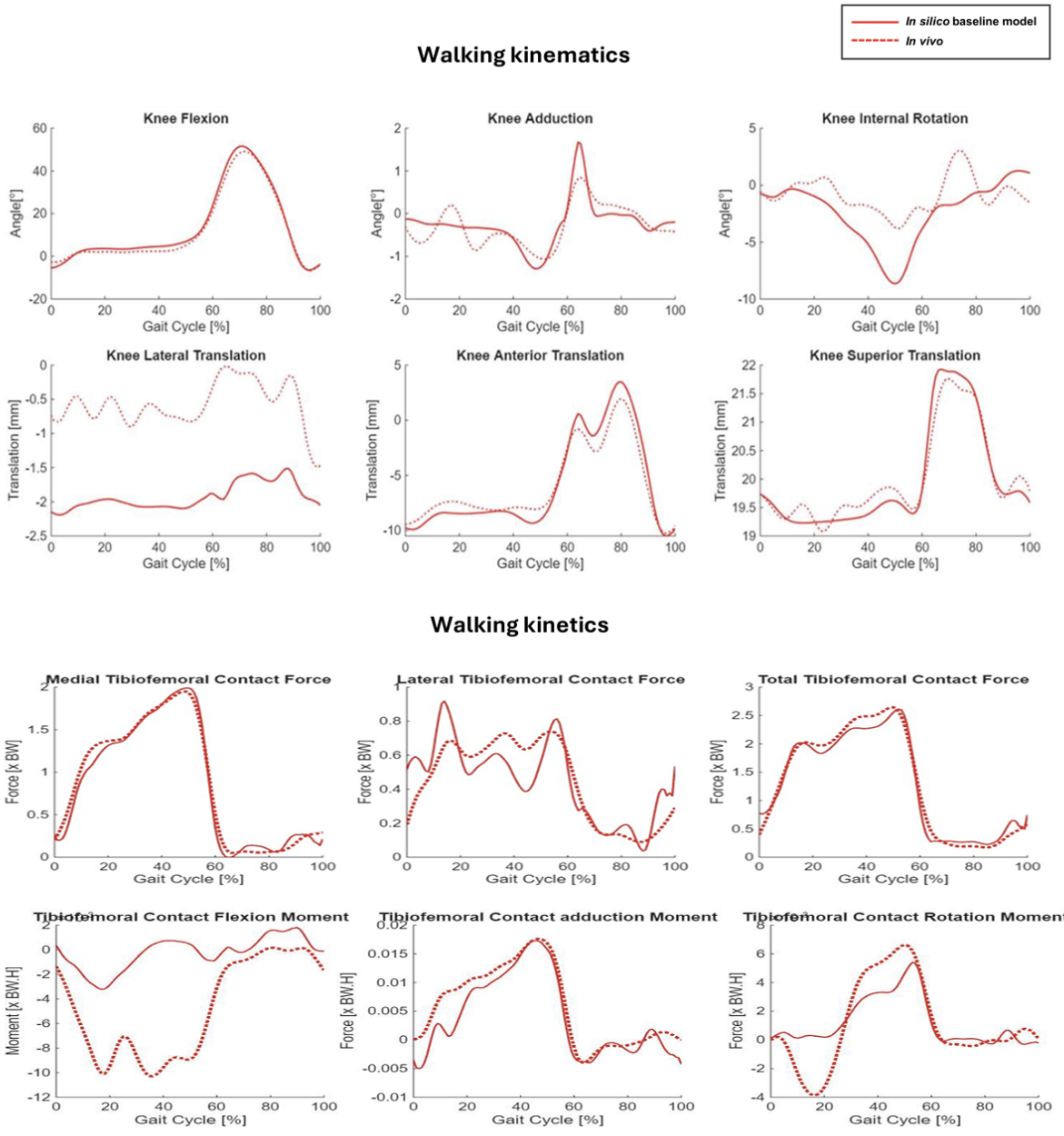

Figure A3: Walking kinematics and kinetics of Cycle 1 *in silico* vs *in vivo* data

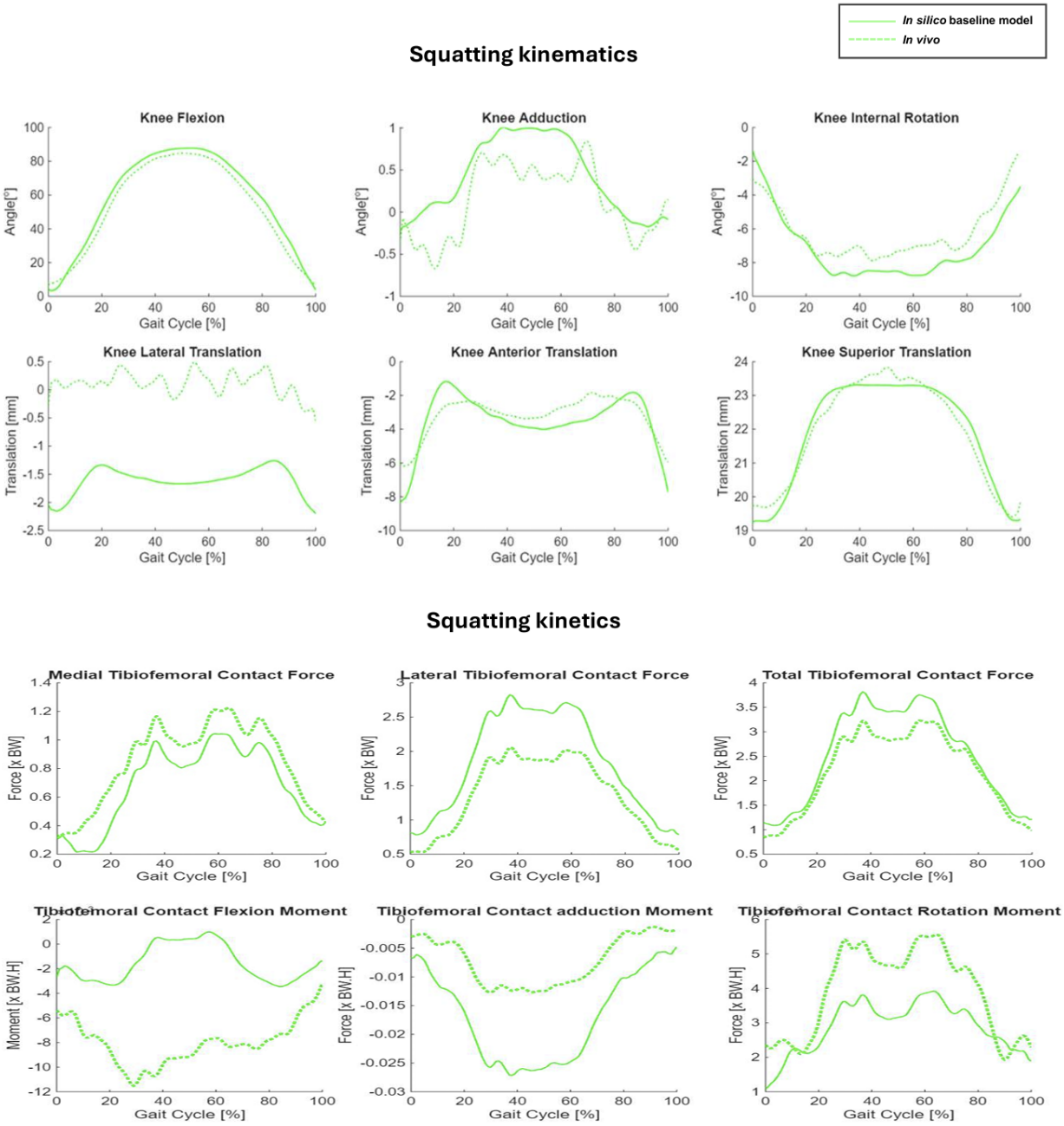

Figure A4: Squatting kinematics and kinetics of Cycle 3 *in silico* vs *in vivo* data.

Abstract in lingua italiana

L'intervento di Artroplastica Totale di Ginocchio (ATG) è considerato il trattamento di riferimento per l'osteoartrite in stadio avanzato, poiché consente di ridurre il dolore e di ripristinare la funzionalità articolare del ginocchio. Nonostante l'elevata sopravvivenza degli impianti, una proporzione significativa di pazienti rimane insoddisfatta a seguito dell'intervento, e diverse combinazioni di taglie dei componenti tibiofemorali sono state indicate come possibili fattori di rischio per la revisione. I chirurghi combinano frequentemente diverse taglie femorali e tibiali per ottimizzare la corrispondenza anatomica; tuttavia, le conseguenze biomeccaniche di tali combinazioni sono ancora poco comprese. In letteratura, diversi studi si sono concentrati su esperimenti *in vitro* o su analisi tramite elementi finiti, focalizzandosi principalmente sulla risposta meccanica degli impianti e fornendo informazioni limitate sulla cinematica articolare durante le attività funzionali. Il presente studio ha impiegato la modellazione muscoloscheletrica per valutare gli effetti di diverse combinazioni di taglie dei componenti tibiofemorali della protesi totale di ginocchio Columbus DD (Aesculap) sulla cinematica e sulla cinetica del ginocchio durante la camminata e lo squat. I modelli muscoloscheletrici consentono di prevedere in modo dinamico e personalizzato i carichi e i movimenti articolari, superando le limitazioni tipiche dei metodi *in vivo* e *in vitro*. I risultati di questo studio hanno mostrato che variazioni di una o due taglie dei componenti tibiofemorali non influiscono in modo sostanziale sulla cinematica del ginocchio né sui carichi di contatto. Sono state tuttavia osservate differenze localizzate nelle pressioni di contatto, suggerendo possibili implicazioni per l'integrità meccanica dell'impianto nel tempo. L'assenza di differenze cinematiche significative è probabilmente legata alla congruenza costante tra tibia e femore del design Columbus DD, che consente la combinazione sicura di diverse taglie femorali e tibiali senza impatti biomeccanici rilevanti. Nel complesso, questo studio rappresenta un buon punto di partenza per future ricerche sulle diverse combinazioni di taglie dei componenti tibiofemorali in ATG e può contribuire a supportare la pianificazione chirurgica finalizzata all'ottimizzazione della scelta di taglia dei componenti, dei relativi risultati clinici e a fornire informazioni utili anche ai fabbricanti.

Parole chiave: ATG, Rischio di revisione, Taglia protesica, Combinazioni di taglie, Modellazione muscoloscheletrica, Columbus DD, Cinematica del ginocchio, Cinetica del ginocchio